INTERNATIONAL JOURNAL FOR NUMERICAL METHODS IN FLUIDS, VOL. 6, 229–240 (1986)

MEASUREMENT OF VELOCITY AND KINETIC ENERGY OF TURBULENCE IN SWIRLING FLOWS AND THEIR NUMERICAL PREDICTION

S. SAMPATH*

Sundaram Clayton Ltd., Padi Madras-50, India

AND

V. GANESAN†

Department of Mechanical Engineering, Indian Institute of Technology, Madras-36, India

SUMMARY

Swirling flows are often employed in gas turbine combustion systems and high intensity industrial furnaces. A detailed analysis of the turbulence in the flow is necessary to achieve optimum combustion conditions. In this paper a method has been described to measure the turbulence levels in three directions using a hot wire anemometer. So far there is no established method available for measurement of turbulence in swirling and recirculating flows.

The present method, it is hoped, will bridge the gap. The merit of the present method is the use of a single-wire probe rather than the X-probe. The method has been used for the measurement of turbulence levels in swirling recirculating flows generated by vane swirlers. From the measured turbulence levels, the kinetic energy of turbulence has been calculated and the results are compared with a well-established numerical prediction method.

Mean velocity measurements have also been made using a 3-hole Pitot probe. The agreement between the measured and predicted values is quite satisfactory.

INTRODUCTION

Because of their high frequency response hot wire anemometers are preferred for the measurement of velocities and turbulence intensities. The basic problem in hot wire anemometry is to relate the measured hot wire voltages to the velocity components. Conventional methods, such as those discussed by Hinze[1] and Champagne and Sleicher,[2] use the time-averaged form of the hot wire response equation. As it is not possible to solve for the velocity components directly by time-averaging the square-root expansion, the expression within the square-root is first expanded into a series and the expressions for the velocity components are derived neglecting the third- and higher-order correlations. In highly turbulent flows, these higher-order correlations are often not negligible and the series expansion may lead to considerable errors. Use of a 3-sensor probe with digital data analysis will enable the determination of the instantaneous velocity components without

* Deputy Chief Engineer.
† Associate Professor.

0271–2091/86/040229–12$06.00

Received 21 June 1985

approximation. But the method is very expensive, and three sensors placed very close to one another are likely to interfere with each other.

In the present work, a general three-dimensional flow is considered, and exact formulae for the quantities $U^2+\bar{u}^2$, $V^2+\bar{v}^2$, $W^2+\bar{w}^2$, $UV+\bar{u}\bar{v}$, $VW+\bar{v}\bar{w}$ and $WU+\bar{w}\bar{u}$ are derived. After determining the mean velocities U, V and W with the help of a three-hole Pitot probe, the turbulence quantities $\bar{u}^2$, $\bar{v}^2$, $\bar{w}^2$, $\bar{u}\bar{v}$, $\bar{v}\bar{w}$ and $\bar{w}\bar{u}$ are determined.

THE PRINCIPLE OF THE METHOD

Consider an inclined wire of angle β lying in the plane $OX'Y'O'$ which makes an angle α with the plane XOY, as shown in Figure 1. It can be shown that the effective cooling velocity U_{eff} for the wire in this position is given by

$$\begin{aligned} U_{\text{eff}}^2 = {} & [(U+u)\cos\alpha\sin\beta + (W+w)\sin\alpha\sin\beta - (V+v)\cos\beta]^2 \\ & + a^2[(U+u)\sin\alpha - (W+w)\cos\alpha]^2 \\ & + b^2[(U+u)\cos\alpha\cos\beta + (W+w)\sin\alpha\cos\beta + (V+v)\sin\beta]^2, \end{aligned} \tag{1}$$

where a and b are the directional sensitivity coefficients of the wire. Usually $\beta = 45°$, and simplifying with this value of β we obtain

$$\begin{aligned} U_{\text{eff}}^2 = {} & (U+u)^2[(1+b^2)(\cos^2\alpha)/2 + a^2\sin^2\alpha] + (V+v)^2(1+b^2)/2 \\ & + (W+w)^2[(1+b^2)\sin^2\alpha/2 + a^2\cos^2\alpha] + (U+u)(V+v)(b^2-1)\cos\alpha \\ & + (V+v)(W+w)(b^2-1)\sin\alpha + (U+u)(W+w)(1-2a^2+b^2)\sin\alpha\cos\alpha. \end{aligned} \tag{2}$$

For a linearized anemometer system, we have,

$$E_{\text{L}} = SU_{\text{eff}},$$

where S is the sensitivity factor to be determined from the calibration of the wire. Squaring:

$$E_{\text{L}}^2 = S^2U_{\text{eff}}^2.$$

As

$$E_{\text{L}} = \bar{E}_{\text{L}} + e, \qquad \text{and} \qquad \bar{E}_{\text{L}}^2 + e^2 = S^2\bar{U}_{\text{eff}}^2, \tag{3}$$

time averaging equation (2) and substituting in (3), we obtain

$$\begin{aligned} (1/S^2)(\bar{E}_{\text{L}}^2 + \bar{e}^2) = {} & (U^2+\bar{u}^2)[(1+b^2)\cos^2\alpha/2 + a^2\sin^2\alpha] + (V^2+\bar{v}^2)(1+b^2)/2 \\ & + (W^2+\bar{w}^2)[(1+b^2)\sin^2\alpha/2 + a^2\cos\alpha] + (UV+\bar{u}\bar{v})(b^2-1)\cos\alpha \\ & + (VW+\bar{v}\bar{w})(b^2-1)\sin\alpha + (UW+\bar{u}\bar{w})(1-2a^2+b^2)\sin\alpha\cos\alpha. \end{aligned} \tag{4}$$

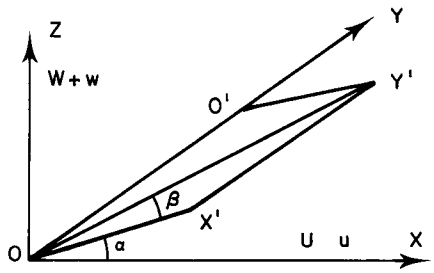

Figure 1. Orientation of the hot wire

If an X-probe is used, for one wire $\beta = 45°$ and for the other wire $\beta = 135°$.

Manfred Bartenwerfer[3] has derived exact formulae for $UV + \bar{u}\bar{v}$, $VW + \bar{v}\bar{w}$ and $UW + \bar{u}\bar{w}$ from the three usual X-wire orientations and $U^2 + \bar{u}^2$, $V^2 + \bar{v}^2$, and $W^2 + \bar{w}^2$ from three suitable orientations which are not symmetrical to each other. This requires the measurements to be made along two different axes. In the present work, measurements are taken with a 45° inclined wire at angles $\alpha = 0$, 45, 90, 180 and 270 degrees with respect to the axis OY. The response equations of the 45° wire can be obtained by substituting the values of α in equation (4). To make the system of equations solvable one more measurement is taken with a straight wire in the plane XOY with the wire parallel to the axis OX. The response equation of the straight wire in this position is

$$U_{\text{eff}}^2 = b_0^2(U + u)^2 + (V + v)^2 + a_0^2(W + w)^2,$$

where a_0 and b_0 are the directional sensitivity coefficients of the straight wire.

Time averaging, we obtain

$$\begin{aligned} U_{\text{eff}}^2 &= b_0^2(U^2 + \bar{u}^2) + (V^2 + \bar{v}^2) + a_0^2(W^2 + \bar{w}^2), \\ (E_L^2 + \bar{e}^2)/s_0^2 &= b_0^2(U^2 + \bar{u}^2) + (V^2 + \bar{v}^2) + a_0^2(W^2 + \bar{w}^2) \end{aligned} \tag{5}$$

The five response equations of the 45° wire and the response equation of the straight wire are solved to determine the quantities $U^2 + \bar{u}^2$, $V^2 + \bar{v}^2$, $W^2 + \bar{w}^2$, $UV + \bar{u}\bar{v}$, $VW + \bar{v}\bar{w}$ and $UW + \bar{u}\bar{w}$. As the mean velocity components U, V and W are determined separately using a three-hole Pitot probe, the turbulence quantities $\bar{u}^2$, $\bar{v}^2$, $\bar{w}^2$, $\bar{u}\bar{v}$, $\bar{v}\bar{w}$ and $\bar{u}\bar{w}$ are readily determined. The percentage turbulences in the axial, radial and tangential directions are then calculated as follows:

$$\begin{aligned} T_u &= \text{percentage intensity in the axial direction} = \sqrt{(\bar{u}^2)}/U_{\text{ref}} \times 100, \\ T_v &= \text{percentage intensity in the radial direction} = \sqrt{(\bar{v}^2)}/U_{\text{ref}} \times 100, \\ T_w &= \text{percentage intensity in the tangential direction} = \sqrt{(\bar{w}^2)}/U_{\text{ref}} \times 100, \end{aligned}$$

where U_{ref} is the inlet velocity.

Once $\bar{u}^2$, $\bar{v}^2$, $\bar{w}^2$ are estimated, kinetic energy of turbulence can be calculated as

$$\text{K.E.} = (1/3)(\bar{u}^2 + \bar{v}^2 + \bar{w}^2)$$

The advantages of the method are

(i) The formulae used in the method are exact, as no approximations have been made.
(ii) The method can be used even for flows with high turbulence intensity.
(iii) The method does not require orienting the probe along the streamline at the point of measurement.

A limitation of the method is that the mean velocities have to be determined by some suitable method. The inaccuracy, if any, in the measurement of the mean velocities will be carried over to the turbulence intensities also. This problem can be overcome to a great extent by using well-calibrated three-dimensional Pitot probes and precision micromanometers for the measurement of mean velocities, as is done in this investigation.

EXPERIMENTAL SET-UP

The experiments were conducted in the wind tunnel set-up shown in Figure 2. The blower in the wind tunnel was driven by a 12 kW constant speed motor running at 2900 r.p.m. The inlet velocity to the system was adjusted using the throttle control at the exit of the blower. The

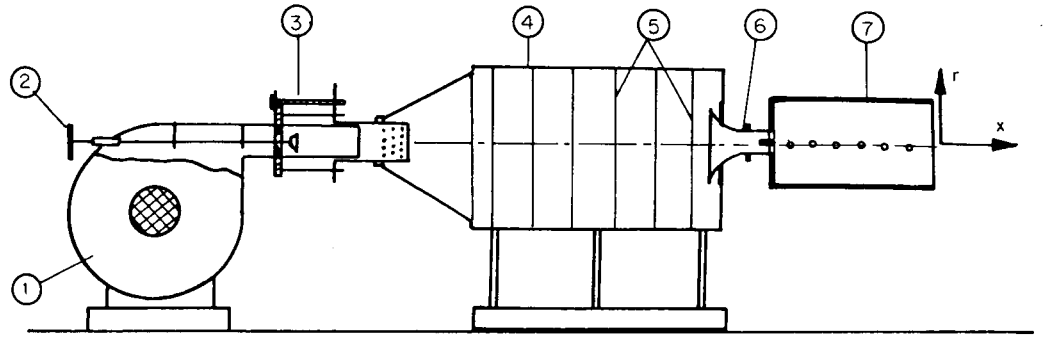

Figure 2. Test set-up: 1 blower; 2 control throttle; 3 bypass control; 4 filter box; 5 filter elements; 6 nozzle; 7 test geometry

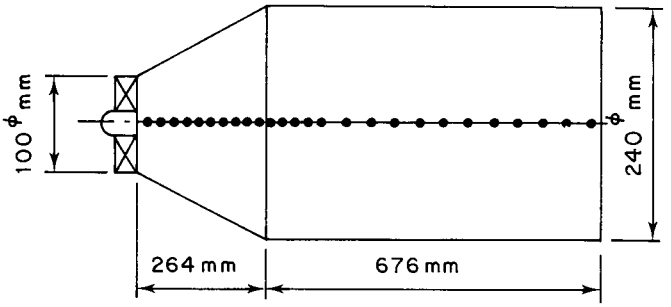

Figure 3(a). Geometry 1

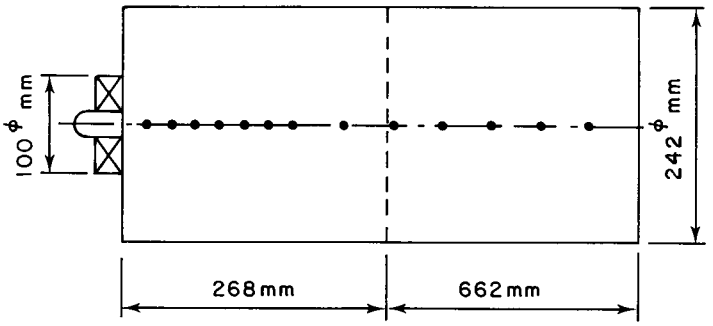

Figure 3(b). Geometry 2

geometries of the systems used for the experiments are shown in Figures 3(a) and 3(b). Air enters the test section through a vane swirler, the details of which are shown in Figure 4. The inlet velocity of air was maintained at 25 m/s. The experiments were conducted at atmospheric pressure and the temperature variations were within $\pm 2°C$.

The mean velocity measurements were made using a three-hole Pitot probe.[4] The turbulence quantities were measured using a constant temperature hot wire anemometer by employing the method described above.

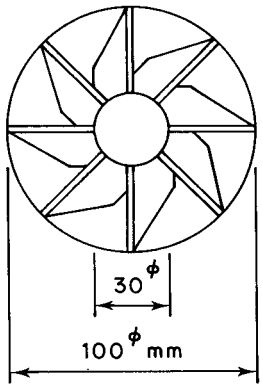

Figure 4. Vane swirler

THEORETICAL STUDY

The predictions were made using a finite difference scheme[5] adapted for recirculating flows. The equations solved for isothermal flows are the continuity equation, U, V and W momentum equations, the equation for turbulence kinetic energy, k, and the dissipation rate (ε) equation. The equations are elliptic in nature and can be presented in the general form:[6]

$$\frac{\partial}{\partial t}(\gamma\phi) + \operatorname{div}(\gamma\bar{\mathbf{v}}\phi - \Gamma \operatorname{grad}\phi) = S$$

where ϕ is the dependent variable, γ is identically equal to either the mixture density ρ or zero, Γ is the appropriate exchange coefficient for the variable and S is the source term, which includes both the sources of ϕ and any other terms which cannot find a place on the left-hand side of the equation or which are required to cancel the effects of some of the terms on the left-hand side.

The differential equations are first reduced to finite difference forms in the manner described in detail by Spalding,[7] and are then solved by the SIMPLE (*S*emi-*I*mplicit *M*ethod for *P*ressure-*L*inked *E*quations) procedure described by Caretto *et al.*[8] and Pun.[9] The main features of the solution procedure are summarized here. The procedure is a semi-implicit iterative one which starts from given initial values of all the variables and converges to the correct solution as the number of iterations increases. For each iteration, the sequence is as follows:

(a) The U and V momentum equations are solved first with guessed pressures.
(b) Since these velocities do not satisfy the continuity equation locally, a 'Poisson-type' correction equation is derived from the continuity equation and from the linearized momentum equations. The 'Poisson' equation is then solved to obtain corrections to the pressure field. The two velocities are then corrected accordingly.
(c) The W momentum equation is then solved.
(d) The kinetic energy k and dissipation rate ε equations are solved for the new values of the velocities.

DETAILS OF THE CALCULATIONS

Grid

Initially 10×10 and 20×10 grids were tried. Finally the chosen grid had 25×12 nodes in the x, r directions, respectively, and the inter-node spacings were non-uniform. A still finer grid

may produce more accurate results. However, it will require large computer storage and time in solving the equations. Further, with a 25 × 12 grid the predicted results were in satisfactory agreement with the measured values.

Convergence

The number of iterations required to provide an acceptably convergent solution was 300. The criteria for convergence include that the magnitude of the residuals in the finite difference equations be less than 1 per cent.

RESULTS AND DISCUSSION

Figures 5 and 6 show the predicted and measured axial velocity distributions at various axial locations for geometries 1 and 2, respectively. The dotted lines indicate the recirculation zone experimentally determined from the locations where flow reversal occurs. From these Figures, it can be seen that close to the swirler the agreement between predicted and measured values

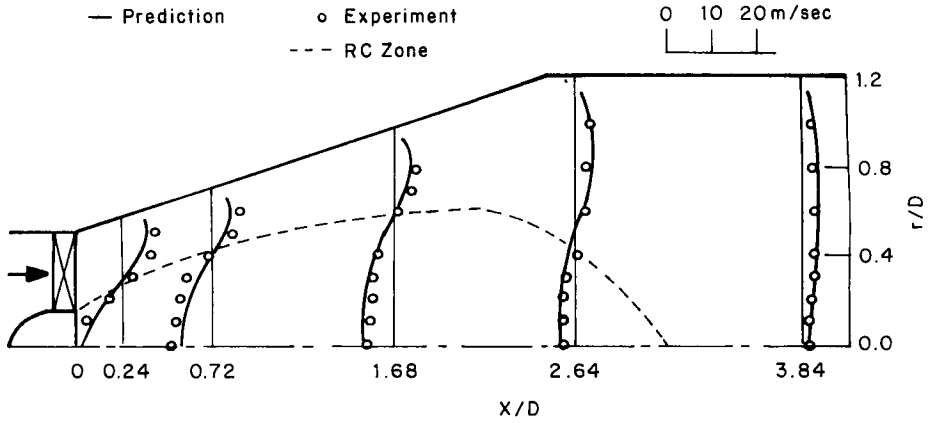

Figure 5. Axial velocity distribution in geometry 1

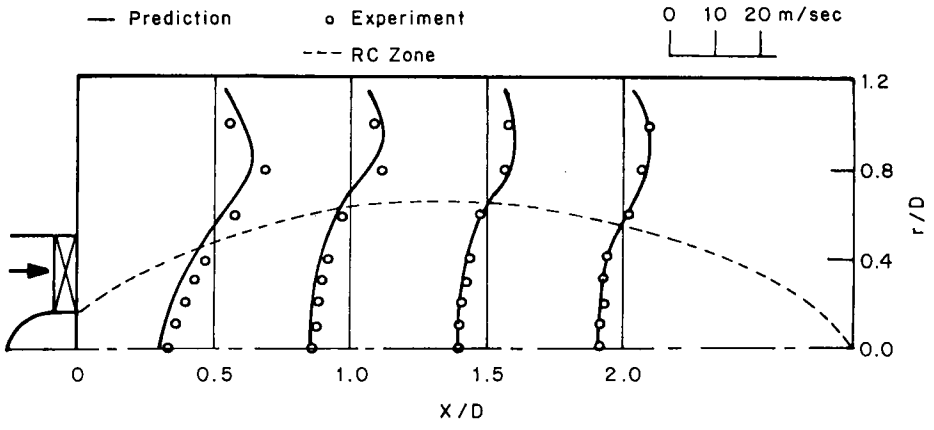

Figure 6. Axial velocity distribution in geometry 2

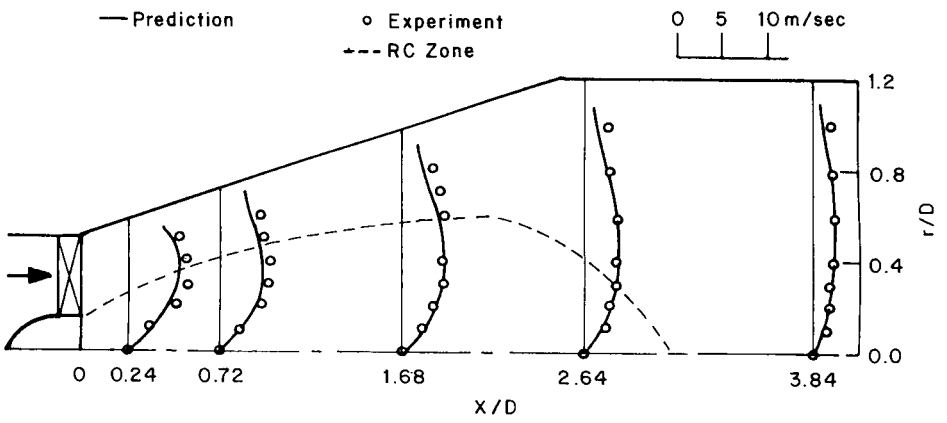

Figure 7. Tangential velocity distribution in geometry 1

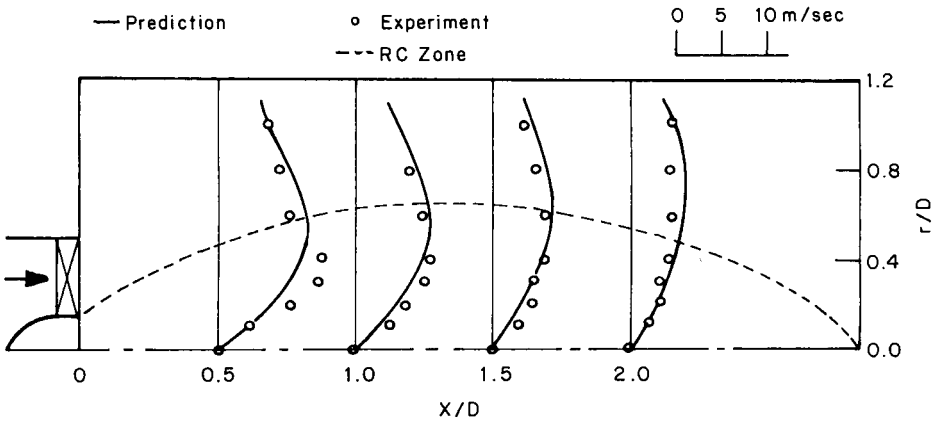

Figure 8. Tangential velocity distribution in geometry 2

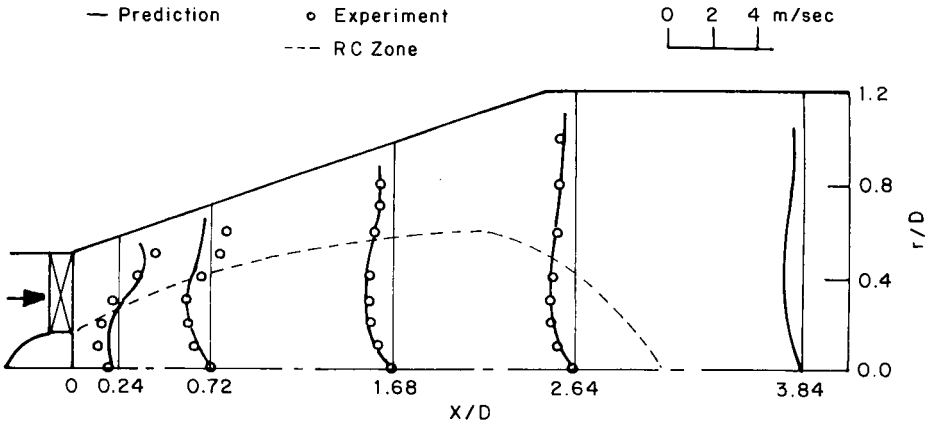

Figure 9. Radial velocity distribution in geometry 1

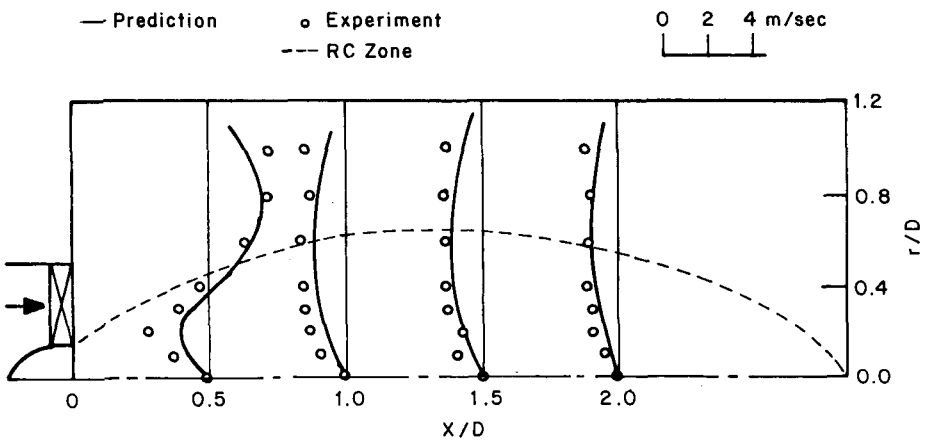

Figure 10. Radial velocity distribution in geometry 2

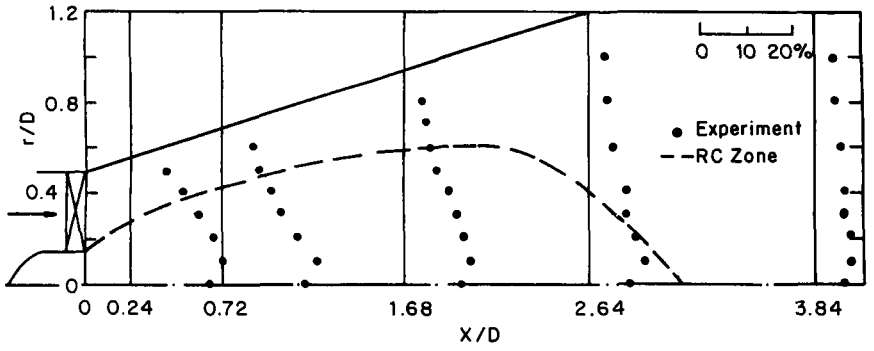

Figure 11. Radial distribution of $T_u = \sqrt{(\bar{u}^2)}/U_{ref}$ in geometry 1

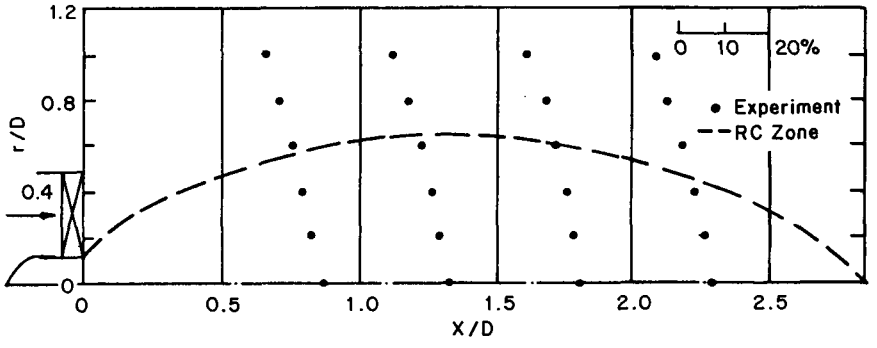

Figure 12. Radial distribution of $T_u = \sqrt{(\bar{u}^2)}/U_{ref}$ in geometry 2

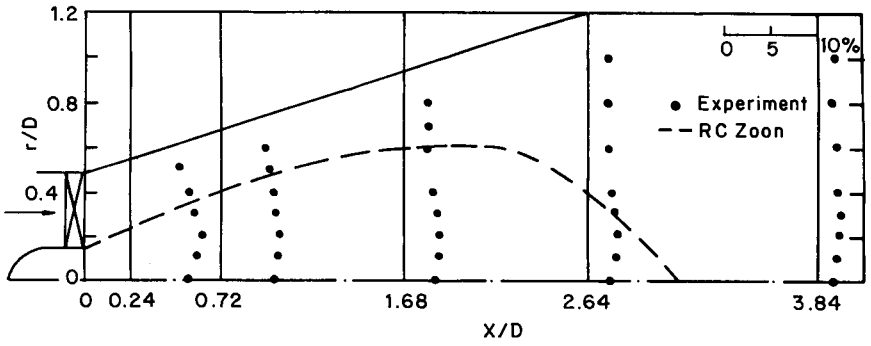

Figure 13. Radial distribution of $T_v = \sqrt{(\tilde{v}^2)}/U_{ref}$ in geometry 1

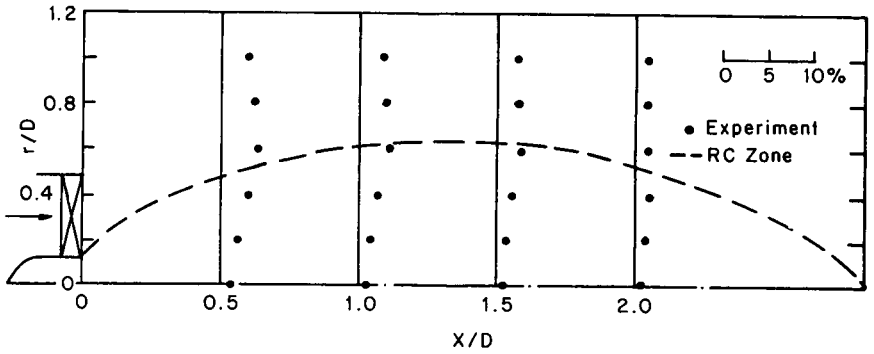

Figure 14. Radial distribution of $T_v = \sqrt{(\tilde{v}^2)}/U_{ref}$ in geometry 2

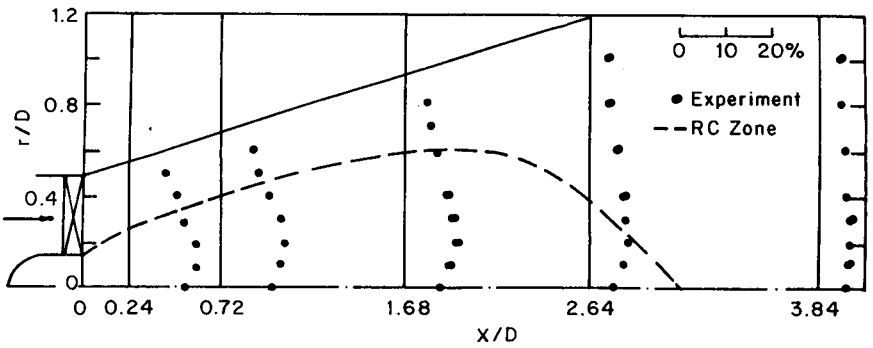

Figure 15. Radial distribution of $T_w = \sqrt{(\tilde{w}^2)}/U_{ref}$ in geometry 1

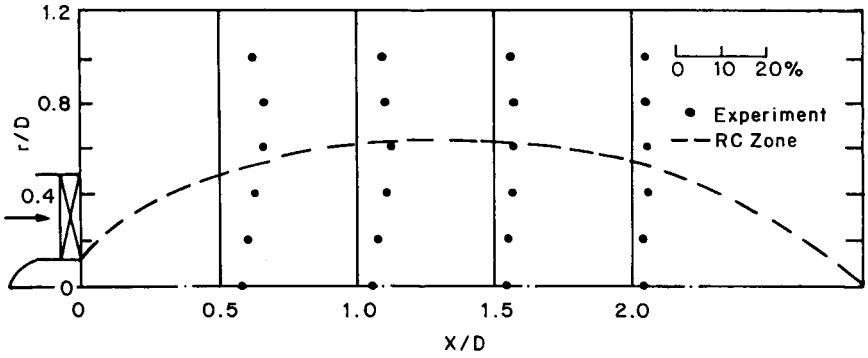

Figure 16. Radial distribution of $T_w = \sqrt{(\bar{w}^2)}/U_{ref}$ in geometry 2

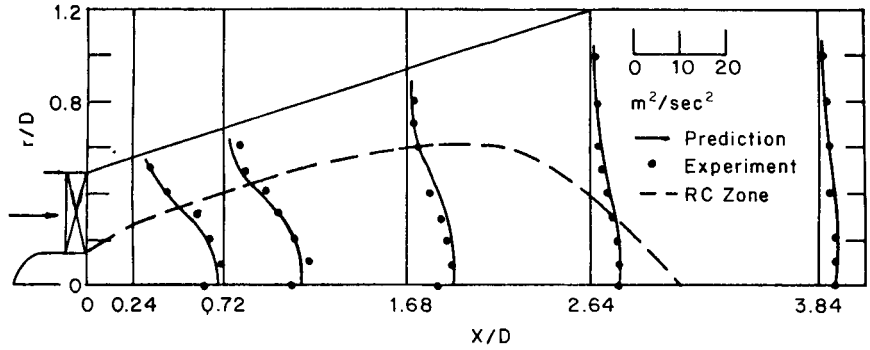

Figure 17. Radial distribution of kinetic energy of turbulence in geometry 1

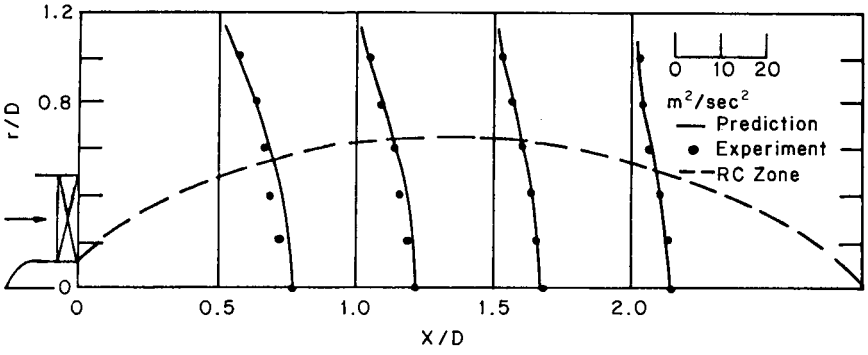

Figure 18. Radial distribution of kinetic energy of turbulence in geometry 2

is not that good compared to the agreement away from the swirler. This may be due to the lack of accurate knowledge of the exact inlet conditions of velocities, swirl intensity, etc.

Figures 7 and 8 show the tangential velocity profiles for geometries 1 and 2, respectively. The tangential velocity close to the axis increases with increase in radius. This indicates the presence of a forced vortex type of motion. With further increase in radius, the profile becomes flat and the tangential velocity starts decreasing towards the wall. The magnitude of the tangential velocity decreases with increase in X/D. The agreement between the predicted and measured values is in general good.

Figures 9 and 10 show the radial velocity profiles for geometries 1 and 2, respectively. The magnitude of the radial velocity is quite small compared to the magnitudes of the axial and tangential velocities. Because of the very small magnitude, accurate measurement is difficult using the Pitot probe, and hence the scatter is more. The magnitude of radial velocity decreases with increase in X/D. Close to the swirler ($X/D < 0{\cdot}5$), the radial velocity changes sign from negative to positive in the radial direction. At locations away from the swirler ($X/D > 0{\cdot}5$) the radial velocity is negative at all radii. The negative value indicates that the radial velocity is towards the axis.

As the magnitude of the radial velocity is small, as already explained, the scatter is more and the agreement between the predicted and measured values is not good, especially close to the swirler. However, the agreement improves with increase in X/D.

Figures 11 and 12 show the measured turbulence intensities (T_u) in the axial direction for geometries 1 and 2, respectively. The turbulence intensity is maximum close to the axis and starts decreasing as radius increases. The turbulence intensity decreases with increase in X/D. This is due to the rapid expansion of the jet and decay in velocity and turbulence.

Figures 13 and 14 show the measured turbulence intensities (T_v) in the radial direction for the two geometries. The turbulence intensity in the radial direction is smaller in magnitude compared to the turbulence intensity in the axial direction.

Figures 15 and 16 show the measured turbulence intensities (T_w) in the tangential direction for geometries 1 and 2, respectively. The maximum value of T_w occurs close to the boundary of the recirculation zone for both the geometries. At any other radius, the value of T_w decreases with increase in X/D, indicating the decay of turbulence.

Figures 17 and 18 shows the predicted and measured profiles of kinetic energy of turbulence for the two geometries considered. It can be seen that the kinetic energy of turbulence is quite high close to the swirler. At any axial location, the kinetic energy of turbulence is maximum close to the axis and decreases as the radius increases. The profiles exhibit a rapid decay of turbulence with the increase of X/D. Agreement between predicted and measured values is not good close to the swirler but improves with increase in X/D.

CONCLUSION

The method illustrated in the present work gives reasonable results in the measurement of turbulent intensities in three-dimensional flows. However, the mean velocities should be determined with sufficient accuracy by other suitable means. This may be considered as a drawback. The predicted results are, in general, in satisfactory agreement with the measured values.

REFERENCES

1. J. O. Hinze, *Turbulence*, McGraw-Hill, New York, 1959.
2. F. H. Champagne and C. A. Sleicher, 'Turbulence measurements with inclined hot wires, part II. Hot wire response equations', *J. Fluid Mech.*, **28**, (1967).

3. M. Bartenwerfer, *Bemerkungen Zur Analyse Von Hitzdrant-singallen stark tiurbulente stromongren*, Deutsche Luft-und Raumfahrt (DLR), Forschongsberiont, 1976.
4. K. Sethuramalingam and Anand R. Menon, 'Recirculation studies in a gas turbine combustion chamber model', *U.G. Project Report*, Dept. of Mech. Engg., I.I.T., Madras, India, 1978.
5. S. V. Patankar and D. B. Spalding, 'A calculation procedure for heat, mass and momentum transfer in three dimensional parabolic flows', *Int. J. Heat and Mass Transfer*, **15**, 1787 (1972).
6. S. Sampath, V. Ganesan and B. H. L. Gowda, 'Use of flow visualization studies in the prediction of flow characteristics in two-dimensional recirculating flows', *J. Institute of Energy*, 321 (1984).
7. D. B. Spalding, 'A novel finite difference formulation for differential equations involving both first and second order derivations', *Int. j. numer. methods eng.*, **4**, 551 (1972).
8. L. S. Caretto, A. D. Gosman, S. V. Patankar and D. B. Spalding, 'Two calculation procedures for steady three dimensional flows with recirculation', *Proc. of the 3rd Conference on Numerical methods in Fluid Mechanics*, vol. 2, 1973, p. 60.
9. W. Pun, 'The air trip computer program', *CHAM Report 591*, 1975.